STRUCTURE AND PROPERTIES OF WELDED JOINTS ON TITANIUM ALLOYS CONTAINING SILICON ADDITIONS

L.I. MARKASHOVA, S.V. AKHONIN, G.M. GRIGORENKO, M.G. KRUGLENKO, A.S. KUSHNARYOVA and **I.K. PETRICHENKO**
E.O. Paton Electric Welding Institute, NASU, Kiev, Ukraine

Structural-phase transformations in specimens of electron beam welded joints on two experimental heat-resistant pseudo- α and $\alpha + \beta$ multi-component titanium alloys containing silicon additions were investigated. Specific (differentiated) contributions of different types of structures and phase formations in the near-weld zone to strength values and distribution of local internal stresses in the welding zones under investigation were analytically estimated.

Keywords: *heat-resistant titanium alloy, structural state, phase formations, microdiffraction reflections, strength characteristics, local internal stresses*

Compared to aluminium alloys, steels and nickel superalloys, high values of strength, specific strength and corrosion resistance of titanium alloys over a wide temperature range favour their increasingly wider application in aircraft and space engineering, ship building, chemical industry, etc. The use of titanium alloys grows due to high reliability of this class of materials at increased and high (of the order of 600–650 °C) temperatures, as well as in high-temperature and aggressive environments, this allowing replacement of parts and components of steels and other structural materials by titanium ones (parts of cases of rocket engines and nuclear power plants, disks and blades of compressors, steam turbines, turbine and gas-turbine engines, heat exchangers, etc.). Heat-resistant titanium alloys are receiving an increasing acceptance in motor car construction, this leading to a substantial increase in power of automobile engines [1–3].

However, complication of service conditions related to increase in the level of working temperatures and necessity to extend the life of parts and mechanisms requires not only improvement of composition and technology of treatment of initial materials, but also finding a solution to the problem of their weldability. The latter is of special importance in manufacture of long and complex-configuration structures, as well as in repair-and-renewal operations, including, for example, reconditioning of worn-out engine blades.

As increase in service properties and level of working temperatures of any structure can be achieved, first of all, by appropriate alloying, as well as by providing the required structural state of the employed metals, alloys and their welded joints, the focus in this study is on conducting more comprehensive investigations of structural-phase changes depending on alloying with silicon, and on evaluating the chemical composition $\rightarrow$ structure $\rightarrow$ properties relationship for titanium alloys and their welded joints.

In this connection, considering the complexity of the processes and mutual effect of alloying and phase formation under different technological conditions of the thermal-deformation effect (welding, heat treatment), it seems expedient not only to perform appropriate experimental studies of structural-phase changes (chemical composition, character of grain, sub-grain and dislocation structure, and phase precipitates differing in composition, morphology and distribution) under certain welding conditions, but also to evaluate the effect of specific structural-phase components on changes in mechanical characteristics of the welded joints that are most significant for service conditions, such as strength, ductility and crack resistance values. This will make it possible to determine the role of structural and phase components not only in strengthening of metal, but also as a factor affecting the processes of accumulation of local internal stresses, value and extent of this type of stresses, as well as the possibility of their plastic relaxation, which is an indicator of crack resistance of a material under service conditions.

Materials and procedures. The investigation objects in this study are electron beam welded (EBW) joints on two heat-resistant multi-component titanium alloys. Both alloys contain silicon as an alloying element, and belong to pseudo-α (alloy 1) and $\alpha + \beta$ (alloy 2) titanium alloys (Table).

The basic experimental information on structural-phase composition of metal of a welded joint was generated by using optical, analytic scanning microscopy (SEM-515, PHILIPS, Holland) and microdiffraction transmission electron microscopy (JEM-200 CX, JEOL, Japan) with accelerating voltage of 200 kV. Thin foils for transmission microscopy were prepared by the two-stage method, i.e. preliminary electropolishing and subsequent multiple ion thinning by ionised argon flows in a specially developed unit [4]. The latter allowed not only widening the investigation fields (increasing statistics), but also making all structural and phase components of a material being analysed «transparent» for electrons.

Investigation results. The optical metallography methods were used to reveal structure, presence and arrangement of cold cracks in the EB welded joints on two experimental titanium alloys in the most problematic zone of a welded joint, i.e. HAZ [5–7], which in fact is a near-weld zone (NWZ), whose size and structure are determined by the thermal cycle of welding, and where the most dramatic changes in structure are expected to take place, allowing for high cooling rates characteristic of EBW.

Cold cracks were found to form in the welded joints on the investigated alloys after welding, the rate of formation of this type of cracks in the welded joints on experimental alloy 1 being much higher (Figure 1, *a*, *b*) than in the welded joints on alloy 2.

Also, as shown by metallographic examinations of structure, coarse equiaxed polyhedral primary β-grains up to 0.5 mm in size form in NWZ of the welded joints on alloy 1 (Figure 1, *c*). In NWZ of the welded joints on alloy 2 the primary structure is heterogeneous: along with large regions of polyhedral grains 0.2 mm in size (Figure 1, *d*), there are regions of fine 20–60 μm equiaxed grains surrounded by coarse grains (Figure 1, *e*). Formation of chains of fine equiaxed grains was observed also in the HAZ regions located at a distance from the weld (Figure 1, *f*). As a rule, they extend along the base metal rolling direction (normal to the weld axis). Often, location of fine grains coincides with localisation of clusters of dispersed precipitates, most probably silicide ones. Intragranular structure in NWZ of alloy 1 consists of a coarse-acicular α′-phase. In NWZ of alloy 2, the martensitic α′-phase has a fine-acicular structure (see Figure 1, *c*, *d*). In addition to the martensitic phase, NWZ of both alloys may contain the retained β-phase, the amount of which, according to the chemical composition, is very insignificant in alloy 1, and higher in alloy 2 than in alloy 1.

More detailed structural-phase examinations of HAZ of the welded joints on titanium alloys by using microdiffraction transmission electron

Chemical composition of experimental heat-resistant alloys

Alloy	Content of alloying elements, wt.%							Coefficient of stability of β-phase K_β
	Al	Sn	Zr	Mo	V	Nb	Si	
1	5.2	3.3	4.2	0.1	0.6	0.8	0.6	0.07
2	4.3	4.4	6.0	1.6	0.7	4.3	0.4	0.33

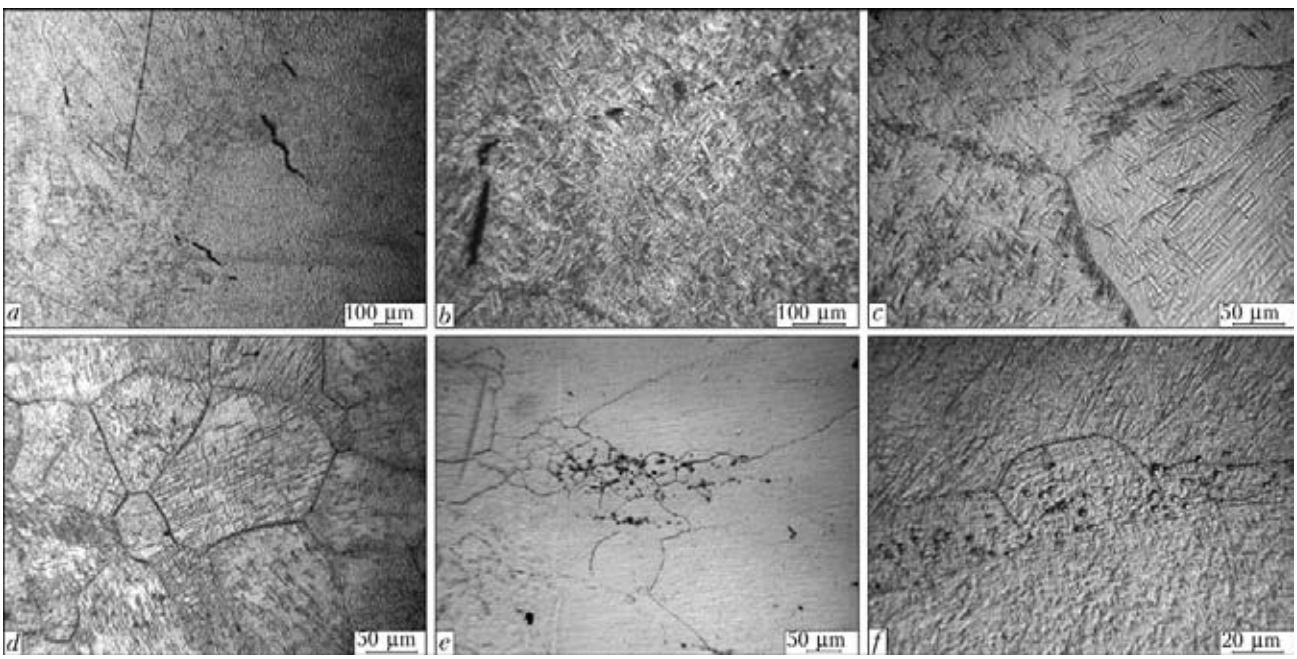

Figure 1. Microstructures of HAZ metal on experimental heat-resistant alloys after EBW: *a*, *b* — alloy 1, cracks in HAZ metal; *c* — alloy 1, NWZ; *d*, *e* — alloy 2, NWZ; *f* — alloy 2, HAZ region located at distance from the weld

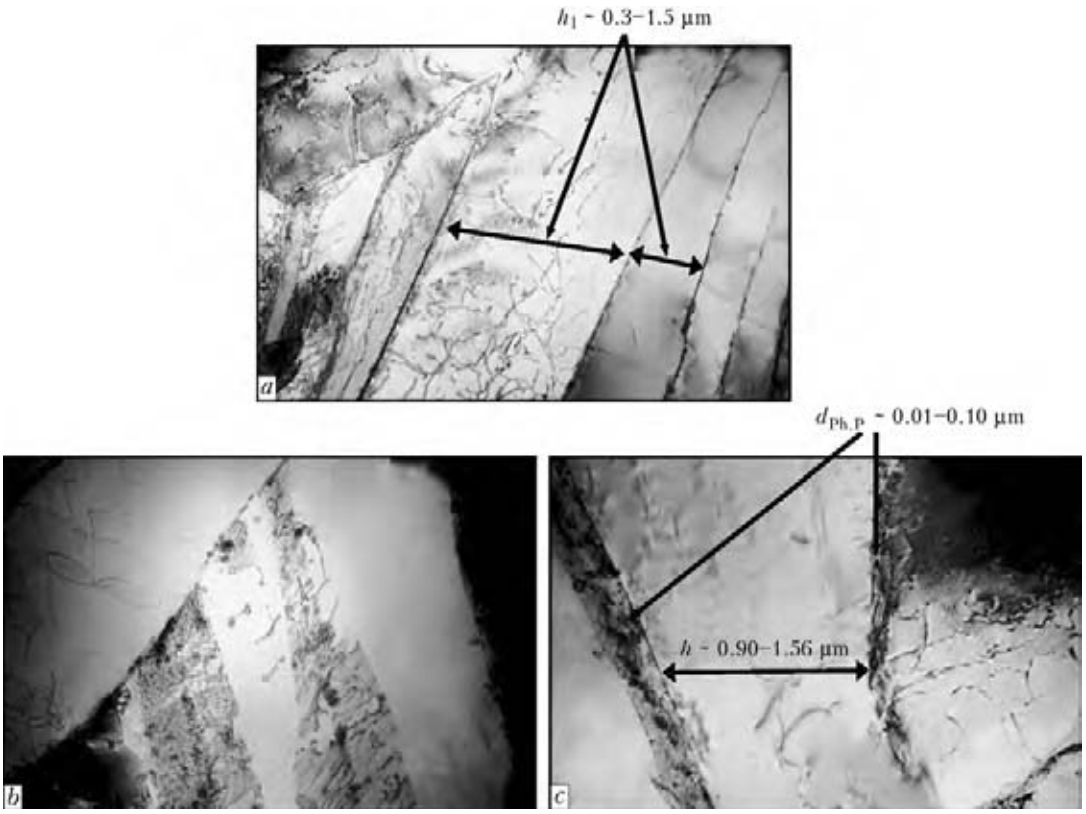

Figure 2. Microstructure of experimental alloy 1, NWZ: *a* — well-defined orientation of laminae of mainly α-component of structure at comparatively low density and uniform distribution of dislocations (lamina width h_l ~ 0.3–1.5 μm), ×20,000; *b*, *c* — phase formation in internal volumes and in boundary regions of α-laminated structures, ×30,000

microscopy were carried out to determine composition of the forming phases, as well as their sizes, morphology and structural zones of their localisation (internal volumes or grain-boundary regions).

Welded joint on experimental heat-resistant alloy 1. Structure of NWZ of the EB welded joint on alloy 1 consists mainly of the laminated α′-phase and a very small amount of the laminated β-phase, which differ in length l_l of a submicron sized (approximately from 0.3 to 1.5 μm) form with cross section h_l (Figure 2, *a*). Moreover, the laminated structural components differ greatly in their internal structure. The major part of this type of structures (consisting mostly of the α′-phase, according to the microdiffraction analysis) is characterised by a minimal dislocation density ($\rho \sim 10^9$ cm^{-2}) in the internal volume of the uniformly distributed laminae. The other part of the laminated structures (their quantity being much lower) radically differs both in dislocation density and distribution. For example, in this type of the laminated structures the dislocation density is higher approximately by an order of magnitude ($\rho \sim (7–8)\cdot 10^{10}$ cm^{-2}). The distribution of crystalline lattice defects in some cases is more or less uniform (Figure 2, *a*, *b*), whereas in other cases the complex dislocation configurations in the form of blocks or cells, as well as an intralaminar dispersed (d_s ~ 0.1 μm) sub-structure (Figure 3, *a*) are detected. The structure with a clearly defined intralaminar substructure is most pronounced in the dark field imaging mode (Figure 3, *c*).

It should be noted that structures with a high dislocation and phase precipitate density correspond not only to the β-phases, but also partially to the α′-phases.

Examinations of thin foils allowed generating the detailed information on the phase precipitates forming in the welded joint, which differ in size, morphology, stoichiometric composition and localisation zones (along the boundaries of the laminated structures, in internal volumes, in substructure, etc.).

Phase precipitates of fine sizes ($d_{Ph.P}$ ~ 0.01–0.10 μm) forming in narrow grain-boundary interlayers and along the interlaminar boundaries (see Figure 2, *c*), the composition of which corresponds mainly to stoichiometry Ti_5Si_3 (Figure 3, *b*), are most distinct. The fine phase precipitates form also in internal volumes of the α′- and β-laminae, in the bulk of which fragmentation of the intralaminar structure and formation of sub-structures take place (Figure 3, *a*–*c*). The phases forming in this type of the structures are detected primarily in the zones of intralaminar sub-structural boundaries, and are characterised

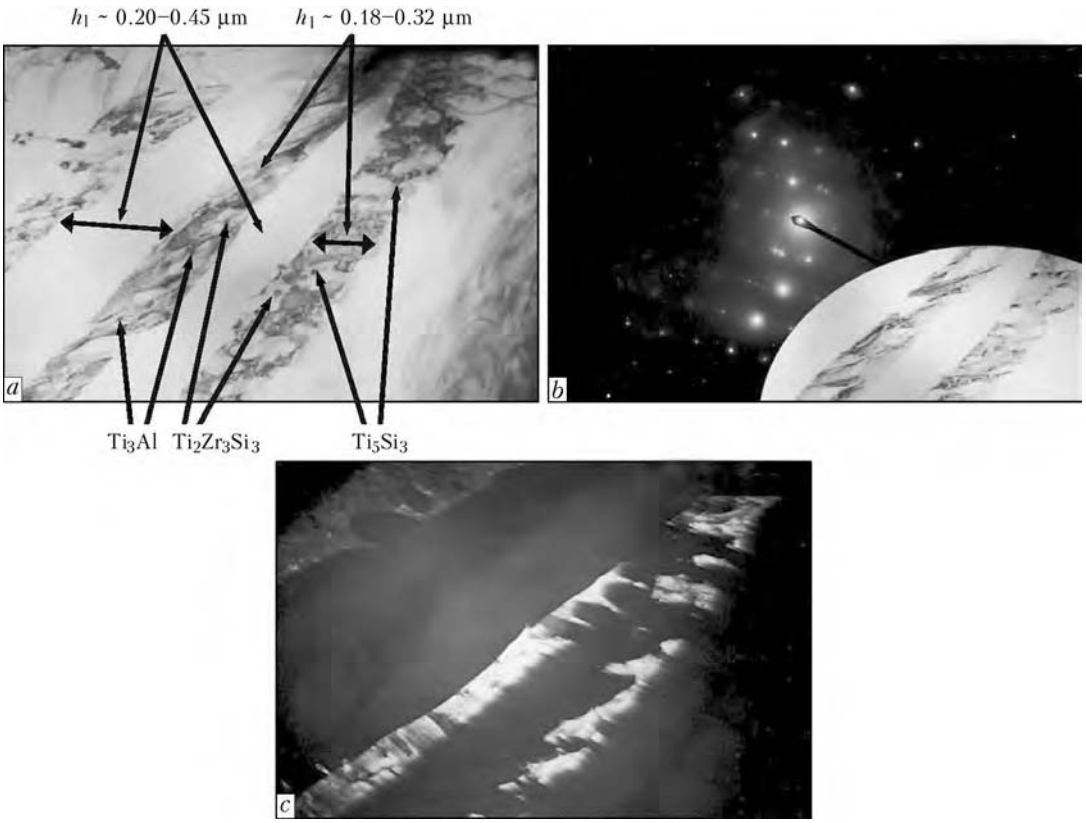

Figure 3. Microstructure of experimental alloy 1, NWZ: *a* — fine structure of laminae with sub-structure, ×37,000; *b* — microdiffraction reflection; *c* — dark-field image of specific (marked with arrows in Figure 3, *a*) phase formations, ×3000

by the finest sizes, i.e. $d_{Ph.P}$ ~ 0.01–0.02 μm. As can be seen, such phases are the phases bordering the sub-structure. In addition to the fine equiaxed phase precipitates, there are also precipitates of an extended form, when $l_{Ph.P} >> h_{Ph.P}$ at l_l ~ ~ 0.7–0.8 μm, propagating along this type of the sub-structural boundaries (Figure 3, *a*, *b*). Stoichiometric composition of the fine phase precipitates bordering the intralaminar sub-structure becomes a bit wider: in addition to the noted Ti_5Si_3 composition, there are also phases of other compositions, including such elements as aluminium and zirconium, i.e. Ti_3Al and $Ti_2Zr_3Si_3$ phases (Figure 3, *a*–*c*; Figure 4, *a*).

The most active development of phase formation is characteristic of the laminated structures of comparatively coarse (in cross section) sizes (h_l ~ 0.4–1.5 μm). Besides, the active phase formation in such zones is accompanied by occurrence of the following important factors. Firstly, coarsening of the phase formations takes place, i.e. size of the phase formations $d_{Ph.P}$ amounts to about 0.1–0.2 μm, this being an order of magnitude higher than size of the intralaminar subboundary phases observed in the laminated structures of a smaller cross section (see Figure 4, *a*). Secondly, no ordering can be seen in distribution of coarse, mainly silicide phases in the bulk of the massive α′-laminae: the forming phases are distributed chaotically, and they are not related either to structural boundaries, or grain and subgrain boundaries. Moreover, formation of intravolume phases in the said cases is accompanied by a substantial increase, i.e. up to $(7–8)\cdot10^{10}$ cm^{-2}, of the dislocation density in the phase formation zone propagating along the entire length of the laminae (Figure 4, *b*, *c*). Therefore, a distinctive feature of the structure of the metal under investigation is formation of extended, special α-lamina structural zones saturated with coarse globular phase precipitates surrounded by dense dislocation clusters.

As follows from the results of investigations of the dislocation structure and phase formation processes, a substantial difference between the structural-phase states of the α′- and β-laminated structures is observed in the welded joints on experimental alloy 1. There occurs parallel formation of the laminated structures dramatically differing in their structural-phase states, such as almost dislocation-free laminae containing no phase precipitates, along with laminae characterised by a high dislocation density and saturation of the internal volumes with chaotically distributed precipitates of a rather coarse size. It is likely that formation of the substantially graded (as to phase precipitates and dislocation density) laminae is attributable to the type of the crys-

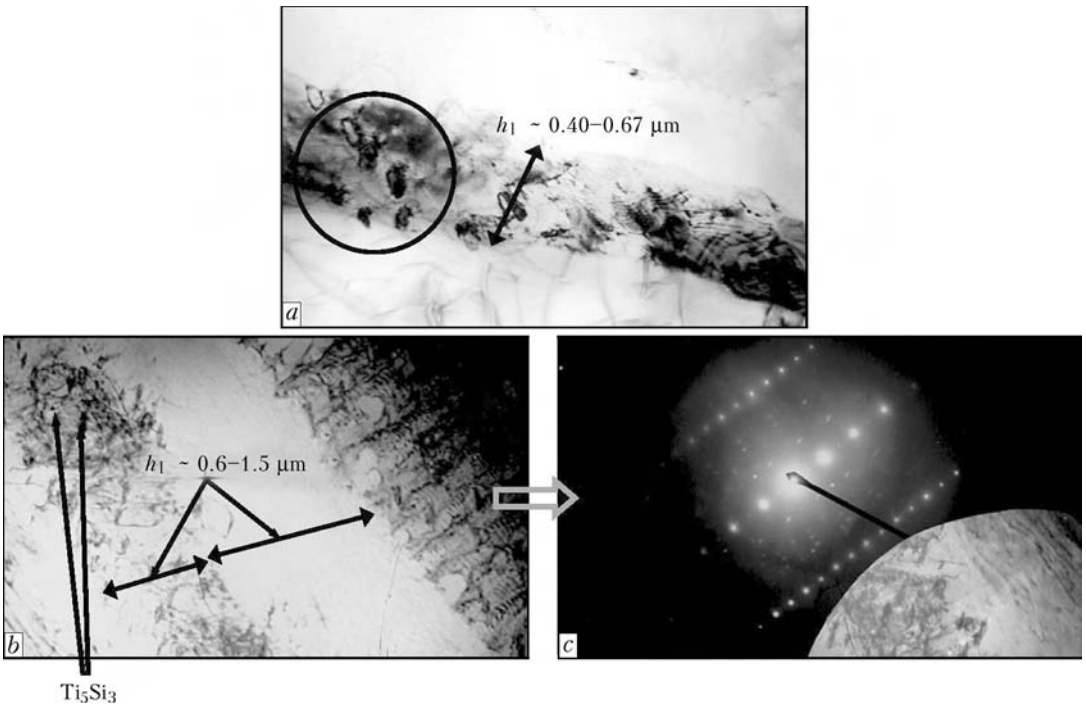

Figure 4. Microstructure of experimental alloy 1, NWZ: *a* — phase formation in β-laminae, ×50,000; *b* — extended dramatic gradients of dislocation density along the laminated structures, ×30,000; *c* — combined microdiffraction reflections of specific phases in α′-lamina structures

talline lattice corresponding to the β- and α-formations in titanium alloys. For instance, the β-phase having the bcc lattice (comprising up to 48 sliding systems) has an almost unlimited possibility for initiation, sliding and redistribution of dislocations, which are known to serve as active channels for transportations of alloying elements and, hence, activation of the phase formation processes. The α-structure having the hcp lattice is characterised by a very limited quantity of the sliding systems. Predominantly, this is one basal (0001) plane, and deformation in metal with this type of the lattice is realised due to twinning, which hampers dislocation initiation and sliding and, therefore, phase formation.

Most probably, it is different peculiarities in realisation of the deformation processes (through dislocation sliding or twinning) and, as a result, different phase formation possibilities for the main phase components (α- and β-phases) that explain formation of the extended laminated structures characterised by sharp gradients of the dislocation density and saturation with phase precipitates. The presence of the graded structural-phase formations, which are substantially different in the quantity and degree of dispersion of the silicide phases, including in dislocation density, is likely to serve as a base for formation in metal of this type of the corresponding sharply graded mechanical characteristics, such as gradients of strength properties ($\sigma_{0.2}$ and σ_t) in the related laminated structures.

Therefore, it was found that NWZ of alloy 1 is characterised by the presence of the extended α′- and β-laminated phase formations, sharply graded in dislocation density, as well as in quantity and size of the forming silicide and intermetallic phase precipitates:

- α′ — laminated phase components (hcp lattice) characterised by a minimal intralaminar dislocation density and an insignificant quantity of phase precipitates in laminae;
- β — laminated structures (bcc lattice) and a small part of the α′-phase characterised by a dramatic increase in the general dislocation density, formation of the sub-structure, very intensive development of the phase formation processes (growth of size and quantity of phases) and distribution of the silicide and intermetallic phases in zones of the dislocation clusters.

Welded joint on experimental heat-resistant alloy 2. Metal structure in NWZ of the EB welded joint on experimental alloy 2, similar to experimental alloy 1, is represented by different phases (α′- and β-phases), which differ both in size and fine structure of the phase formations and in size and distribution of the silicide and intermetallic precipitates originating during the welding process.

For example, cross section size h_l of laminae of the martensitic α′-phase is much smaller (approximately 2–3 times) compared to that of the laminated structures of the corresponding zone of the welded joint on experimental alloy 1, and

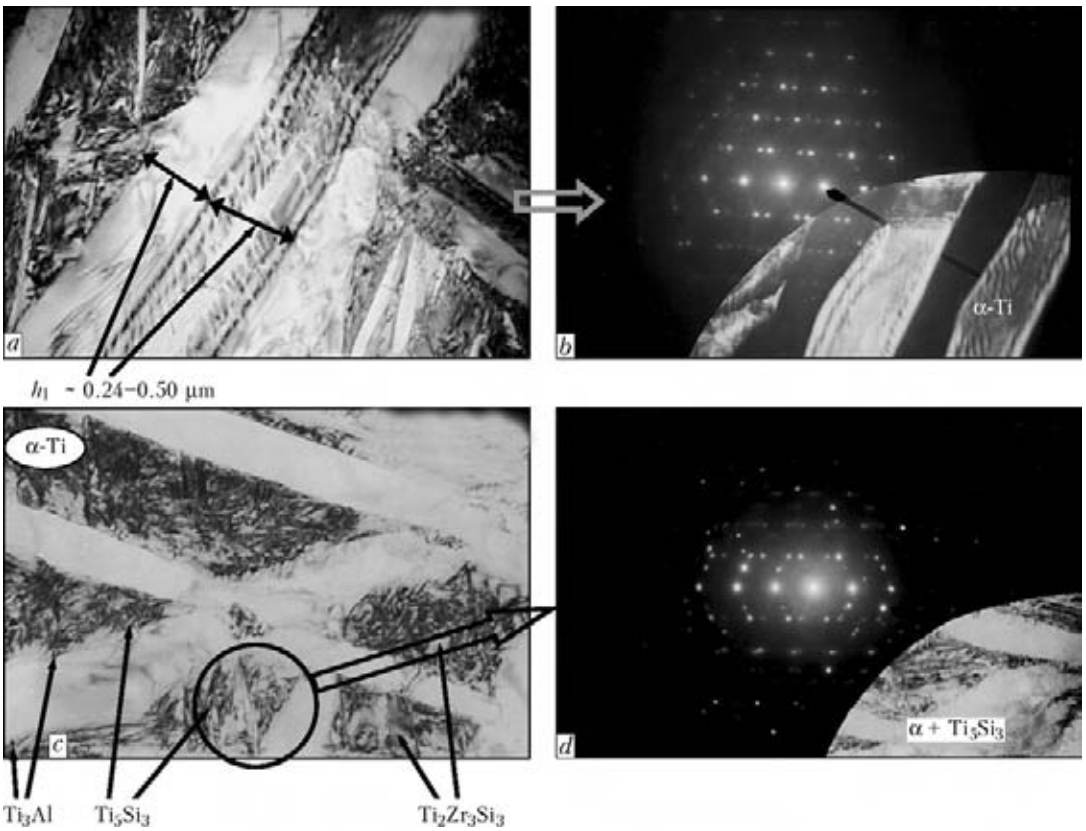

Figure 5. Microstructure of experimental alloy 2, NWZ: *a*, *c* — fine structure of laminated phases of the martensitic type (*a* — ×50,000; *c* — ×37,000); *b*, *d* — microdiffraction reflections of phase precipitates

is equal to 0.2–0.5 μm (Figure 5, *a*). In addition, no dramatic changes in thickness of the laminae are observed. In this case, and this should be emphasised, structure of the α′- and β-phases is characterised by the presence of the acicular and fine intralaminar sub-structure. The dislocation density equal to $\rho \sim (8–9)\cdot 10^{10}$ cm^{-2} is uniformly distributed.

As to the phase precipitates, structural examinations and parallel analysis of microdiffraction reflections (Figure 5, *b*, *d*; Figure 6, *b*, *d*) show formation of primarily fine (0.01–0.02 × 0.02–0.06 μm) and comparatively more uniformly distributed silicide and intermetallic phases in NWZ of the welded joint on alloy 2, compared to the welded joint on alloy 1. Moreover, the forming phases are distributed mainly in internal volumes of the laminated structures, first of all along the sub-structural boundaries, i.e. they are phase precipitates that border the intralaminar sub-structural elements (Figures 5 and 6). This character of distribution of the fine phase precipitates should promote not only fixation of the formed intralaminar sub-structure, but also consolidation of the thus fixed structure up to a temperature of dissolution of the grain-boundary distributed phases. Besides, this type of the structural state (fine fragments with grain-boundary fixing phases) is more or less uniformly distributed in the entire volume of the NWZ metal.

Analysis of microdiffraction reflections of the structures being investigated reveals diversity of stoichiometric compositions of the phase precipitates forming in NWZ of the joints on alloy 2. These are mostly phases of the Ti_5Si_3, $Ti_2Zr_3Si_3$ and Ti_3Al types (Figure 5, *d*; Figure 6, *b*). As seen, compositions of the precipitated silicides and intermetallics hardly differ from those detected in NWZ of the welded joint on alloy 1. However, morphology of this type of the phases, their size and distribution are substantially different. In the welded joint on alloy 2, silicides and intermetallics are finer, have a rod-like or globular shape (see dark-field image in Figure 6, *b*), and are distributed more uniformly in the bulk of metal, which seems to be caused by a structural state of the NWZ metal of the welded joint on this alloy, i.e. by a comparatively more uniform and finer structure of α′-martensite. However, despite a more favourable change in structural-phase state of the NWZ metal on alloy 2, including dispersion and uniformity of structure, formation of fine precipitates along the structural boundaries and absence of the laminated structure that is dramatically graded in its structural-phase state, the presence of a pronounced extension of the laminated structures will lead, though to a smaller degree (compared to the NWZ state in alloy 1), to decrease in

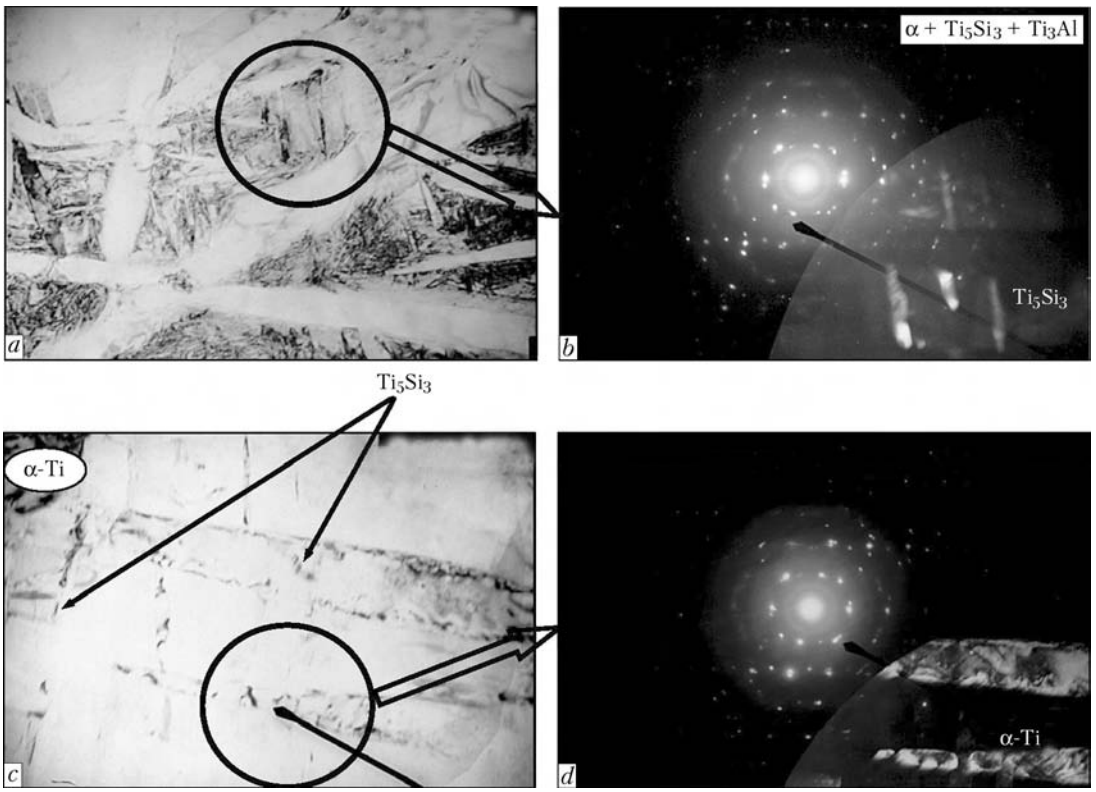

Figure 6. Microstructure of experimental alloy 2, NWZ: *a*, *c* — distribution of phase precipitates differing in morphology and size, ×50,000; *b*, *d* — microdiffraction reflections of specific zones of phase precipitates

ductility values and, accordingly, to increase in susceptibility of the welded joint to cracking.

Therefore, NWZ of the welded joint on experimental alloy 2 is characterised by formation of the extended phases of the laminated type (α′-martensite and β-phase) having, like in alloy 1, a laminated morphology, but considerably differing (approximately 2–3 times) in width of the laminated structures, finer acicular α′-martensitic structure and intralaminar sub-structure, as well as more uniform distribution of dislocations in the entire volume of the NWZ metal.

Differences are observed also in the process of formation of the silicide and intermetallic phases: at a similar stoichiometric composition (like in case of alloy 1) the phases are smaller in size and are uniformly distributed in the entire volume, their localisation occurring mainly along the sub-structure boundaries.

Additional fractographic examinations of fractures of the EB welded joints on experimental

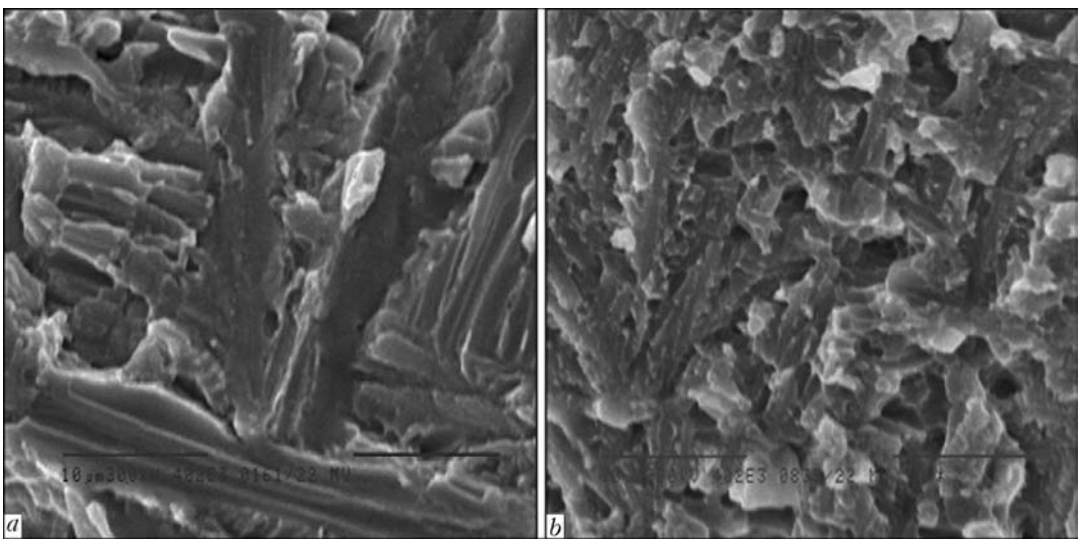

Figure 7. Microstructures of fracture surfaces on titanium alloys (×4020): *a* — brittle cleavage in laminated structures with intravolume phase precipitates (welded joint on experimental alloy 1); *b* — quasi-brittle fracture in martensitic component (welded joint on experimental alloy 2)

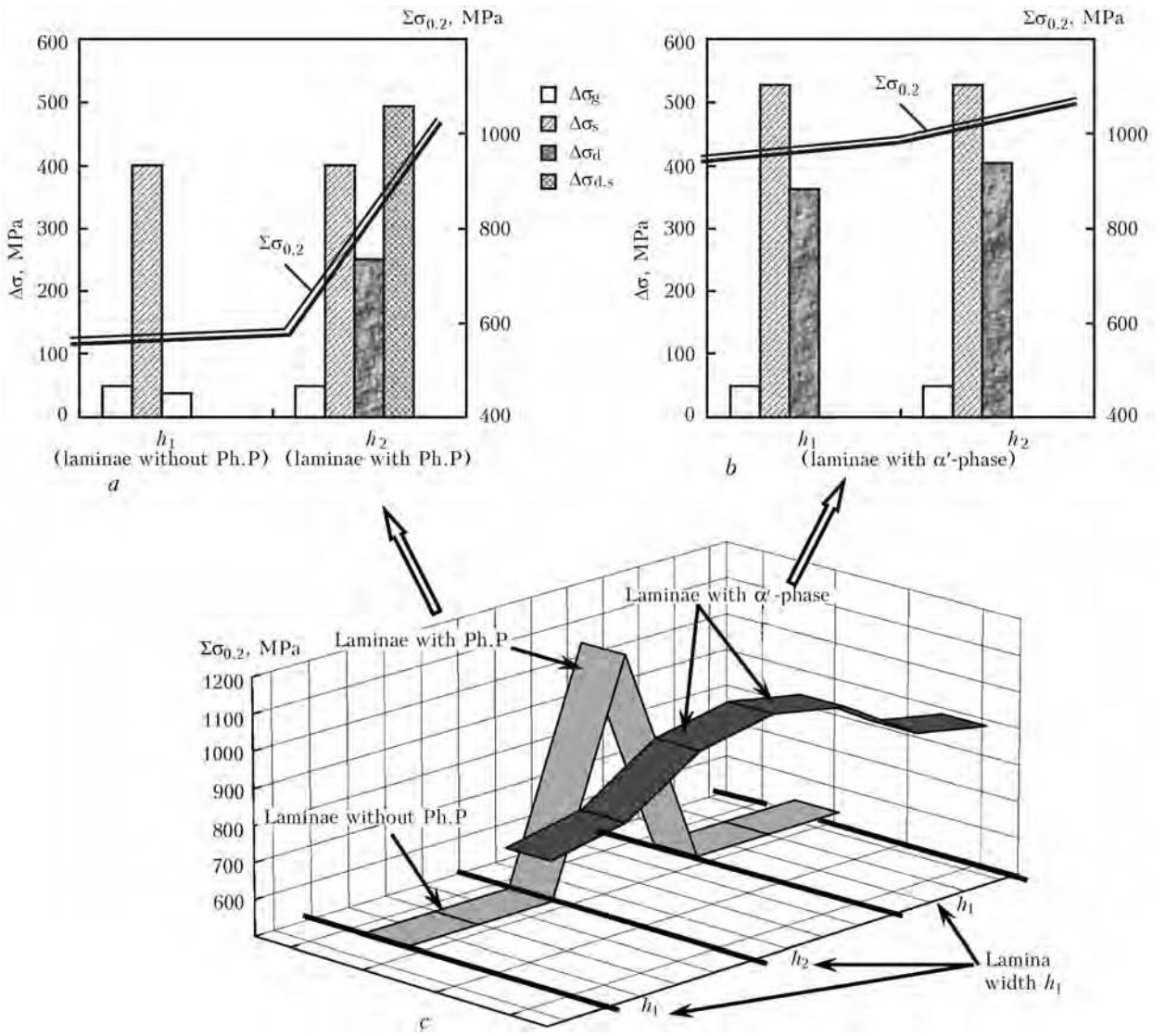

Figure 8. Contribution of different components of structural strengthening (grain, sub-grain, dislocation and dispersion): *a* — alloy 1; *b* — alloy 2; *c* — calculated value of yield strength $\Sigma\sigma_{0.2}$

alloys 1 and 2 showed that the fracture zone of the welded joints on experimental alloy 1 is characterised by the presence of regions of the extended transcrystalline brittle cleavage in a direction of the laminated structures (Figure 7, *a*). In contrast to this, the welded joints on experimental alloy 2 feature a more homogeneous quasi-brittle fracture of the intragranular type (Figure 7, *b*) with dispersed fragments (d_f ~ 2–5 μm) corresponding in size to sub-structural components in α′-martensite.

A substantial effect on quality of the welded joint is exerted by distribution and localisation of internal stresses in the HAZ metal of the alloys investigated. Stresses of this type related to non-uniformity of heating and structural-phase transformations lead to a dramatic decrease in ductility, and in some cases to cold cracking, which occurs under the conditions of EBW of experimental heat-resistant alloys. Therefore, analysis of the role of different structural factors inducing or blocking formation of internal stresses is also of an important practical interest.

The package of the conducted experimental studies made it possible, firstly, to analytically estimate specific (differentiated) contributions of different structural-phase factors and parameters forming in welded joints of the investigated alloys to changes in strength characteristics $\sigma_{0.2}$, and, secondly, to reveal the structural factors determining the character and distribution of internal stresses τ_{in}, which are potential sources of initiation and propagation of cracks in the investigated structural microregions [8–12].

Analytical estimates of strength $\sigma_{0.2}$ were made according to the Archard equation that includes the known Hall–Petch, Orowan and other dependences [13–20]:

$$\Sigma\Delta\sigma_{0.2} = \Delta\sigma_0 + \Delta\sigma_{s.s} + \Delta\sigma_g + \Delta\sigma_s + \Delta\sigma_d + \Delta\sigma_{d.s},$$

where $\Delta\sigma_0$ is the resistance of the metal lattice to movement of free dislocations (friction stress

of the lattice or Peierls–Nabarro stress); $\Delta\sigma_{s.s}$ is the strengthening of solid solution with alloying elements and impurities (solid solution strengthening); $\Delta\sigma_g$, $\Delta\sigma_s$ is the strengthening due to a change in size of grain and sub-grain (Hall–Petch dependences, grain and sub-grain strengthening); $\Delta\sigma_d$ is the dislocation strengthening caused by the inter-dislocation interaction; and $\Delta\sigma_{d.s}$ is the strengthening provided by the dispersed particles according to the Orowan dependence (dispersion strengthening).

It was shown as a result that the HAZ metal of the welded joint on experimental alloy 1 features the dramatically graded (approximately 1.8 times) change in yield strength ($\Delta\sigma_{0.2}$ ~ 570–1010 MPa) that depends on the structural-phase state of the laminated structures. A dramatic increase in $\Delta\sigma_{0.2}$, which is characteristic of the laminated structures with a high dislocation density ($\rho \sim (7–8)\cdot10^{10}$ cm^{-2}) and most saturated with the phase precipitates, leads to a growth of dislocation ($\Delta\sigma_d$ ~ 250 MPa) and dispersion ($\Delta\sigma_{d.s}$ ~ ~ 375–500 MPa) strengthening (Figure 8, *a*, *c*).

NWZ of alloy 2 is characterised by a high level and more uniform distribution of strength properties ($\Delta\sigma_{0.2}$ ~ 910–1040 MPa) in the forming martensitic phases of the laminated type (Figure 8, *b*, *c*), this being related to their finer structure. In this case, a certain increase in strengthening is caused by dispersion of the substructure ($\Delta\sigma_s$ ~ 530 MPa), and a comparatively uniform increase in general dislocation density in the bulk of metal leads to strengthening of an order of $\Delta\sigma_d$ ~ 360 MPa (Figure 8, *b*).

Furthermore, internal stresses τ_{in} in HAZ of the joints were determined by examinations of the dislocation structure [21, 22]:

$$\tau_{in} = Gbh\rho/[\pi(1 - \nu)],$$

where G is the shear modulus; b is the Burgers vector; $h = 2\cdot10^{-5}$ cm is the foil thickness; ν is the Poisson ratio; and ρ is the dislocation density.

The investigations conducted showed (Figure 9, *a*) that the HAZ metal of alloy 1 is characterised by a dramatically graded (approximately 10 times) distribution of internal stresses, directed along the laminae (from 10–100 to 750–860 MPa), this being related to a change of the dislocation density in different types of the laminae, i.e. with low ($\rho \sim 10^9–10^{10}$ cm^{-2}) and high ($\rho \sim (7–8)\cdot10^{10}$ cm^{-2}) dislocation densities. However, there are also regions with an even higher local dislocation density ($\rho \sim 2\cdot10^{11}$ cm^{-2}), where local internal stresses $\tau_{in/l}$ amount to about 2000 MPa.

HAZ of alloy 2 is characterised by a comparatively uniform distribution of internal stresses

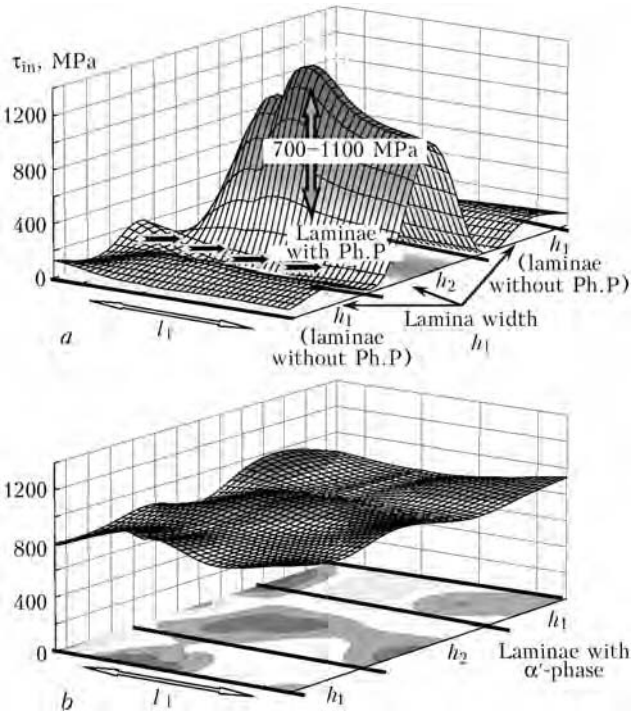

Figure 9. Level of local internal stresses forming in laminated structures of NWZ of the welded joints: *a* — laminated structures graded in distribution of dislocation density, and intravolume phase precipitates (experimental alloy 1); *b* — martensitic laminated structures (experimental alloy 2)

(τ_{in} ~ 860–970 MPa), this corresponding to a uniform dislocation density ($\rho \sim (8–9)\cdot10^{10}$ cm^{-2}) in the intralaminar structures (Figure 9, *b*).

However, both welded joints on alloy 1 and welded joints on alloy 2 (though to a lower degree) feature a clear relationship of orientation of the distribution of internal stresses and the laminated structures, which can be a cause of formation and propagation of cracks.

CONCLUSIONS

1. As established in the course of the comprehensive investigations of the welded joints on experimental titanium alloys conducted at different structural levels (grain, sub-grain, dislocation), NWZ of the joints on alloys 1 and 2 is characterised by formation of the laminated-type extended structures of the α′- and β-phase components with a similar morphology, but considerably differing in density and distribution of dislocations, as well as in intensity of the processes of formation of phase precipitates of the silicide and intermetallic types.

2. In NWZ of the welded joint on pseudo- α alloy 1, the silicide phase formation occurs most actively in few grains of the β-phase and in a small part of the α′-laminae, which are characterised by a high dislocation density and formation of a sub-structure. At the same time, the

major part of the α′-laminae is characterised by a low dislocation density, uniform distribution of dislocations and absence of silicides and intermetallics in their bulk. Phase precipitates are observed both in the grain-boundary interlayers and along the boundaries between the laminae.

3. The presence of the structural-phase formations in NWZ of alloy 1, which are considerably different in quantity and degree of dispersion of the silicide phases, and in dislocation density, is a base for formation of dramatically graded strength characteristics, as well as internal stresses in the adjoining laminated structures.

4. NWZ of the welded joints on (α + β) titanium alloy of the martensitic type is characterised by formation of finer silicide and intermetallic phase precipitates in the α′- and β-phases, which are mainly uniformly distributed in the bulk of the NWZ metal, i.e. along the sub-boundaries and boundaries of the fine martensitic α′-phase.

5. Analytical estimation of differentiated contribution of different structural-phase factors and parameters forming in the welded joints on the investigated alloys to changes in strength properties ($\sigma_{0.2}$) showed that a substantial change in yield strength $\sigma_{0.2}$ of the adjoining laminated structures occurs in NWZ of the welded joints on alloy 1, i.e. from 570 MPa for the laminated α′-phase with a low dislocation density to 1010 MPa for the laminae with a high dislocation density and silicide precipitates. NWZ of alloy 2 features a higher level and more uniform distribution of strength properties ($\sigma_{0.2}$ changes from 910 to 1040 MPa in the entire volume of the NWZ metal).

6. Estimation of changes in internal stresses τ_{in} in NWZ of the welded joints on the investigated alloys, made on a base of examinations of the dislocation structures, showed that distribution of internal stresses in NWZ of the welded joint on alloy 1 is extremely non-uniform and directed along the laminated structures (τ_{in} changes from 10–100 to 750–860 MPa in the laminae with a high and low dislocation densities). Internal stresses in NWZ of the welded joint on alloy 2 are distributed more uniformly. However, fixation of the direction of the distribution of internal stresses and laminated structures can serve as a cause of a directed propagation of cracks.

7. To eliminate strength and internal stress gradients, it is necessary to achieve formation of a homogeneous uniform dispersed structure.

1. Iliin, A.A., Kolachev, B.A., Polkin, I.S. (2009) *Titanium alloys. Composition, structure, properties*: Refer. book. Moscow: VILS–MATI.
2. Solonin, O.P., Glazunov, S.G. (1976) *Refractory titanium alloys*. Moscow: Metallurgiya.
3. Chechulin, B.B., Ushkov, S.S., Razuvaeva, I.N. et al. (1977) *Titanium alloys in machine-building*. Moscow: Mashinostroenie.
4. Darovsky, Yu.F., Markashova, L.I., Abramov, N.P. et al. (1985) Procedure of thinning of dissimilar welded joint samples for microscopic examinations. *Avtomatich. Svarka*, **12**, 60.
5. Grabin, V.F. (1975) *Principles of metals science and heat treatment of titanium alloy welded joints*. Kiev: Naukova Dumka.
6. Moiseev, V.N., Kulikov, F.R., Kirillov, Yu.G. et al. (1979) *Titanium alloy welded joints*. Moscow: Metallurgiya.
7. Gurevich, S.M., Zamkov, V.N., Blashchuk, B.E. et al. (1986) *Metallurgy and technology of welding of titanium and its alloys*. Kiev: Naukova Dumka.
8. Markashova, L.I., Grigorenko, G.M., Poznyakov, V.D. (2009) Influence of thermal cycles of welding and external loading on structural-phase variations and properties of joints of 17Kh2M steel. *The Paton Welding J.*, **7**, 18–25.
9. Markashova, L.I., Grigorenko, G.M., Arsenyuk, V.V. et al. (2002) Criterion of evaluation of mechanical properties of dissimilar material joints. In: *Proc. of Int. Conf. on Mathematical Modeling and Information Technologies in Welding and Related Processes* (16–20 Sept. 2002, Katsiveli, Ukraine). Kiev: PWI, 107–113.
10. Markashova, L.I., Grigorenko, G.M., Poznyakov, V.D. et al. (2004) Structural approach to evaluation of mechanical properties in HAZ of steel and alloy joints. In: *Proc. of Int. Conf. on Mathematical Modeling and Information Technologies in Welding and Related Processes* (13–17 Sept. 2004, Katsiveli, Ukraine). Kiev: PWI, 174–179.
11. Markashova, L.I., Grigorenko, G.M., Poznyakov, V.D. et al. (2008) Structural factors determining the properties of strength, plasticity and fracture of welded joints. In: *Proc. of Int. Conf. on Mathematical Modeling and Information Technologies in Welding and Related Processes* (27–30 May 2008, Katsiveli, Ukraine). Kiev: PWI, 87–94.
12. Markashova, L.I., Grigorenko, G.M., Poznyakov, V.D. et al. (2009) Structural criterion for evaluation of strength, plasticity, crack resistance of metals, alloys, composite materials and their welded joints. In: *Proc. of 4th Int. Conf. on Fracture Mechanics of Materials and Strength of Structures* (June 2009, Lviv, Ukraine). Lviv: FMI, 447–451.
13. Suzuki, H. (1967) About yield strength of polycrystalline metals and alloys. In: *Structure and mechanical properties of metals*. Moscow: Metallurgiya.
14. Ashby, M.F. (1986) About Orowan stress. In: *Physics of strength and plasticity*. Moscow: Metallurgiya.
15. Goldshtein, M.I., Litvinov, V.S., Bronfin, B.M. (1986) *Physics of metals of high-strength alloys*. Moscow: Metallurgiya.
16. Conrad, H. (1973) Model of deformation strengthening for definition of grain size effect on metal flow stress. In: *Ultrafine grain in metals*. Ed. by L.K. Gordienko. Moscow: Metallurgiya.
17. Armstrong, R.V. (1973) Strength properties of metals with ultrafine grain. *Ibid*.
18. Petch, N.J. (1953) The cleavage strength of polycrystalline. *J. Iron and Steel Inst.*, **173**, 25–28.
19. Orowan, E. (1954) *Dislocation in metals*. New York: AIME.
20. Ashby, M.F. (1983) Mechanisms of deformation and fracture. *Adv. Appl. Mech.*, **23**, 117–177.
21. Koneva, N.A., Lychagin, D.V., Teplyakova, L.A. et al. (1986) Dislocation-disclination sub-structures and strengthening. In: *Theoretical and experimental investigation of disclinations*. Leningrad: LFTI.
22. Conrad, H. (1963) Effect of grain size on the lower yield and flow stress of iron and steel. *Acta Metallurgica*, **11**, 75–77.